Pharm Res (2015) 32:2301–2309
DOI 10.1007/s11095-015-1621-6

RESEARCH PAPER

NMR Spectroscopic and Quantum Mechanical Analyses of Enhanced Solubilization of Hesperidin by Theasinensin A

Ruge Cao • Yutaro Kobayashi • Airi Nonaka • Yuji Miyata • Kazunari Tanaka • Takashi Tanaka • Toshiro Matsui

Received: 30 September 2014 / Accepted: 5 January 2015 / Published online: 10 January 2015

ABSTRACT

Purpose The use of hesperidin in the pharmaceutical field is limited by its aqueous insolubility. The effects of natural compounds in tea on the solubility of hesperidin were evaluated and the underlying mechanism was investigated by nuclear-magnetic resonance (NMR) and quantum mechanical calculations.

Methods The solubility of hesperidin was measured by liquid chromatography time-of-flight mass spectrometry; the structure of the hesperidin/theasinensin A complex was characterized by ^{1}H-NMR, diffusion-ordered NMR spectroscopy, and rotating frame NOE spectroscopy, as well as theoretically by quantum mechanical calculations.

Results Among the natural compounds in tea, theasinensin A was the most effective in improving hesperidin solubility. The complexation of hesperidin with theasinensin A led to changes in the chemical shift of protons in hesperidin ($\Delta\delta$: 0.01–0.27 ppm) and diffusion coefficient (ΔD: 0.66–1.32 $\times$ 10^{-10} m^2/s) of hesperidin. ROE correlation signals between hesperidin and theasinensin A and quantum mechanical calculations revealed that two hesperidin molecules formed a stable complex with theasinensin A (2:1 complex) with a ΔG energy of −23.5 kJ/mol.

Conclusions This is the first study that provides insight into the enhanced solubility of hesperidin through interactions with theasinensin A *via* a 2:1 complex formation between hesperidin and theasinensin A.

KEY WORDS hesperidin · NMR · quantum mechanical calculation · solubility · theasinensin A

ABBREVIATIONS

CAF	Caffeine
CD	Cyclodextrin
D value	Diffusion coefficient value
D_2O	Deuterium oxide
DMSO-d_6	Dimethyl sulfoxide-d_6
DOSY-NMR	Diffusion-ordered-NMR spectroscopy
DSS-d_6	3-Trimethylsilyl-1-propanesulfonic acid-d_6
EGC	(−)-Epigallocatechin
EGCG	(−)-Epigallocatechin-3-*O*-gallate
Hesp	Hesperidin
Nrtn	Narirutin
QM	Quantum mechanical
ROESY	Rotating frame NOE spectroscopy
TSA	Theasinensin A
TSB	Theasinensin B

INTRODUCTION

Hesperidin, an abundant and inexpensive by-product of citrus cultivation and the major flavonoid in orange and lemon peels (1), possess varying pharmacological activities such as anti-

Electronic supplementary material The online version of this article (doi:10.1007/s11095-015-1621-6) contains supplementary material, which is available to authorized users.

R. Cao • Y. Kobayashi • A. Nonaka • T. Matsui (✉)
Division of Bioresources and Biosciences, Faculty of Agriculture, Graduate School of Kyushu University, 6-10-1 Hakozaki, Higashi-ku, Fukuoka 812-8581, Japan
e-mail: tmatsui@agr.kyushu-u.ac.jp

Y. Miyata
Nagasaki Agricultural and Forestry Technical Development Center, Higashisonogi Tea Research Station, 1414 Nakano-go, Higashisonogi, Nagasaki 859-3801, Japan

K. Tanaka
Department of Nutrition, University of Nagasaki, 1-1-1 Manabino, Nagayo, Nagasaki 851-2195, Japan

T. Tanaka
Graduate School of Biochemical Sciences, Nagasaki University, 1-14 Bukyo-machi, Nagasaki 852-8521, Japan

inflammatory, analgesic, hypolipidemic, and anti-cancer (2–4). It has also been shown to have protective effects against cardiovascular and neurodegenerative diseases (5–8). Drug solubility and stability are two very important factors with respect to drug administration and delivery (9). However, the poor solubility of hesperidin in water restricts its bioavailability (10) and negatively affects its efficacy in medical applications. It has also gained significant interest in pharmacy, pharmacology, and biochemistry. For example, Kometani *et al.* developed transglycosylated hesperidin using cyclodextrin (CD) glucanotransferase to glycosylate hesperidin for enhanced solubility (11), while Majumdar *et al.* reported that enhanced solubility could be obtained by inclusion in β-CD (12). Recently, we reported that the solubility of hesperidin could be improved by a fermented tea extract containing black tea polyphenols (13); a ca. 6-fold higher solubility of hesperidin by the fraction of oxidative dimers of catechins (theasinensins and theaflavins) in the extract was obtained compared to that of hesperidin dissolved in water. However, the mechanism underlying the enhanced solubility, in addition to the identity of the responsible component in black tea remains unclear.

Thus, the aim of the present study was to identify the tea polyphenol that enhanced the solubility of hesperidin using liquid chromatography time-of-flight mass spectrometry (LC-TOF/MS). We also evaluated the intermolecular interactions between hesperidin and the tea component in water by ^{1}H-, diffusion-ordered (DOSY)-, and rotating frame nuclear Overhauser effect (ROESY)-NMR, in addition to quantum mechanical (QM) calculations.

MATERIALS AND METHODS

Materials

Hesperidin, caffeine (CAF) and (−)-epigallocatechin-3-*O*-gallate (EGCG) were purchased from Nacalai Tesque Inc. (Kyoto, Japan). Theasinensins A and B (TSA and TSB) were prepared according to previously reported methods (14, 15). Briefly, a solution of EGCG incubated with $CuCl_2$ and ascorbic acid was applied to a Diaion HP20 column (Mitsubishi Chemical Co., Tokyo, Japan), followed by a stepwise elution with methanol to obtain TSA (14). TSB was alternatively obtained by a chromatographic separation of a fermented tea extract produced by tea-rolling processing of a mixture of green tea and loquat leaves (15). The internal standard (IS), 3-trimethylsilyl-1-propanesulfonic acid-d_6 (DSS-d_6, 98.0 atom% D), was obtained from Santa Cruz Biotechnology Inc. (Texas, USA). Deuterium oxide (D_2O, 99.8 atom% D) was acquired from Acros Organics (Fair Lawn, USA). Dimethyl sulfoxide-d_6 (DMSO-d_6, 99.9 atom% D) was obtained from Kanto Chemical Co. (Tokyo, Japan). Other reagents were of analytical grade and were used without further purification.

LC-TOF/MS Measurements

In order to evaluate the solubility, hesperidin and mixtures of hesperidin and CAF, EGCG, TSB, and TSA (denoted as Hesp-CAF, Hesp-EGCG, Hesp-TSB, and Hesp-TSA, respectively) were dissolved in 10% DMSO or water at molar ratio of 1:1, 1:5 and 1:10. After incubating at 37°C for 24 h, the mixtures were centrifuged at 10000*g* for 10 min at 20°C. The obtained supernatants were subjected to LC-TOF/MS. An Agilent 1200 series HPLC (Agilent Technologies, Waldbronn, Germany) equipped with a micro degasser (G1379B), binary pump (G1312A), high performance autosampler SL (G1367B), and a thermostatically controlled oven (G1316A) was utilized. Separation was achieved on a Cosmosil $5C_{18}$-MS-II column (2.0 × 150 mm, Nacalai Tesque Inc., Kyoto, Japan) at 40°C. The mobile phase consisted of 0.1% formic acid (A) and methanol with 0.1% formic acid (B) using a 20 min-linear gradient from 0 to 100% of solvent B, at a flow rate of 0.2 mL/min. MS analysis was performed on a micro TOF-II mass spectrometer (Bruker Daltonics, Bremen, Germany). Electrospray ionization (ESI) was applied and ionization was performed in negative mode. Mass spectral data were collected within the range of 100–1000 m/z, and hesperidin was detected at $[M\text{-}H]^-$ of 609.18 m/z with the width of 0.05 m/z. The ionization conditions were as follows: nebulizer pressure, 1.6 bar; dry gas flow (nitrogen), 8.0 L/min; drying temperature, 200°C; and capillary voltage, 3800 V. TOF/MS was externally calibrated daily using a sodium formate solution containing 10 mM sodium hydroxide in water-acetonitrile (1:1, *v*/*v*).

^{1}H-NMR Measurements

In an attempt to investigate the underlying mechanism of the enhanced solubility of hesperidin, hesperidin was dissolved in 10% DMSO-d_6 and was analyzed by NMR. After incubation at 37°C for 1 h, an aliquot of the sample was placed into a 5 mm-NMR sample tube (Nihonseimitsu Scientific Co., Tokyo, Japan). All measurements were carried out on an ECS-400 spectrometer (JEOL, Tokyo, Japan) operating at 400 MHz and 25°C. ^{1}H-NMR spectra were acquired by a single pulse sequence with water suppression using presaturation under the following conditions: acquisition time, 2.18 s; X offset, 4.7 ppm; acquisition point, 16,384; scans, 16; relaxation delay, 15 s; auto-gain and spinning. The 90° pulse-width of hesperidin was determined using a single pulse sequence under the conditions described above at pulse-width settings from 41.0 to 44.0 μs linearly with 0.1 μs intervals. The spin-lattice relaxation delay (T_1) was measured by an arrayed experiment using an inversion-recovery pulse sequence (16)

with a relaxation delay of 30 s. All spectra were referenced to DSS-d_6 at 0 ppm. Auto-shimming for each measurement was performed with field-gradient shimming at 4 scans at receiver gain of 20. NMR data acquisition and analysis were performed using Delta software (version 1.1).

DOSY Measurements

DOSY NMR measurements using a spin-echo method (17, 18) were performed as described previously using a diffusion time of 0.1 s, field gradient pulse-width of 1.0×10^{-3} s at 256 scans of 16,384 acquisition points, 90° pulse-width of 10.5 μs, and relaxation delay of 30 s at 25°C. By changing the listed grad_1_amp values and evaluating the resulting signal decay of hesperidin, a pulse field gradient was optimized: array type, logarithmic; range, 1.0×10^{-4}–5.0×10^{-1} T/m; and point, 16. The diffusion coefficient (D) value was calculated according to Eq. (1): (19)

$$D = -\frac{1}{(\gamma G\delta)^2\left(\Delta - {}^{\delta}/_{3}\right)}\ln\frac{I(G,\Delta)}{I(0,\Delta)} \quad (1)$$

in which γ is the gyromagnetic ratio in the observation of the nuclei, G is the pulse-field gradient strength, δ is the pulse-width of the field gradient, Δ is the diffusion time, and I is the signal intensity. DSS-d_6 was used as the IS. The D value of hesperidin was normalized to that of IS.

ROESY Measurements

ROESY spectra were acquired under the following conditions: 90° pulse width, 10.5 μs; mixing time, 0.25 s; X offset, 4.7 ppm; X points, 1024; Y points, 256; scans, 48; relaxation delay, 1.5 s.

Quantum Mechanical (QM) Calculations

Quantum mechanical (QM) calculations of the hesperidin-tea component structure in water were performed *via* computational simulations. The initial structures of hesperidin and the tea component were built by Chem3D ver.8.0 (Cambridge Science Computing, Inc., Cambridge, USA). The atom type and chirality were assigned by Sybyl-X.2.1 (Tripos, Inc., St. Louis, USA).

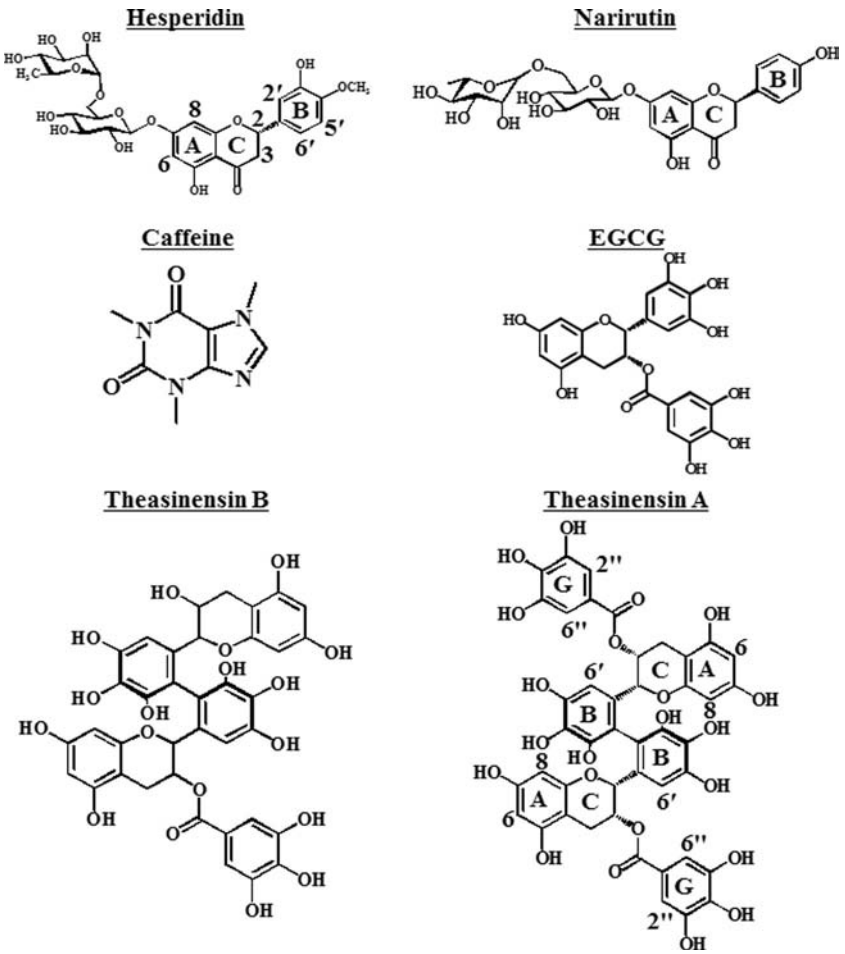

Fig. 1 Chemical structures of hesperidin, narirutin, caffeine, (−)-epigallocatechin-3-*O*-gallate (EGCG), theasinensin B, and theasinensin A used in this study.

All calculations were performed using Gaussian 09. The structure was optimized using a long-range corrected density functional CAM-B3LYP (20) with the cc-pVDZ basis set in the dielectric model of water (polarizable continuum model, PCM) (21) with a dielectric constant of 78.36. The optimized conformations of hesperidin and the tea component were used to determine the conformation of the complex using Gaussview 5.0. The Gibbs free energy (ΔG, kJ/mol) of the complex formation was calculated as the intermolecular energy between hesperidin and tea component.

Statistics

LC-TOF/MS analysis was conducted in triplicate to obtain the solubility data, which were expressed as mean ± standard deviation (SD). Statistical differences among the groups were analyzed by one-way analysis of variance (ANOVA), followed by *post-hoc* Tukey-Kramer's *t*-test analysis. A p value of <0.05 was considered to be statistically significant. All analyses were performed using a Stat View J 5.0 (SAS Institute, Cary, NC, USA).

RESULTS

Solubility of Hesperidin with Polyphenols by LC-TOF/MS Analysis

The chemical structures of hesperidin and typical tea polyphenols used in this study are shown in Fig. 1, where TSB and TSA are EGCG-(−)-epigallocatechin (EGC) dimer and EGCG dimer, respectively. Figure 2a shows the solubility profiles of hesperidin in 10% DMSO with CAF, EGCG, TSB, and TSA at 1:1, 1:5, and 1:10 molar ratios. A concentration dependent increase in the solubility of hesperidin was observed upon combination with TSA. Specifically, at a molar ratio of 1:10, a ca. 3-fold significant ($p<0.05$) increase in the solubility of hesperidin was observed, while only a 2.1-fold increase was observed upon combination with TSB. Furthermore, a 1.6-fold increase was observed with EGCG and a 1.4-fold increase was observed with CAF. A similar enhancement by TSA was also observed in water (Fig. 2b), suggesting that solvent (DMSO)-induced solubilization of hesperidin may be excluded in the enhanced solubility of hesperidin by TSA.

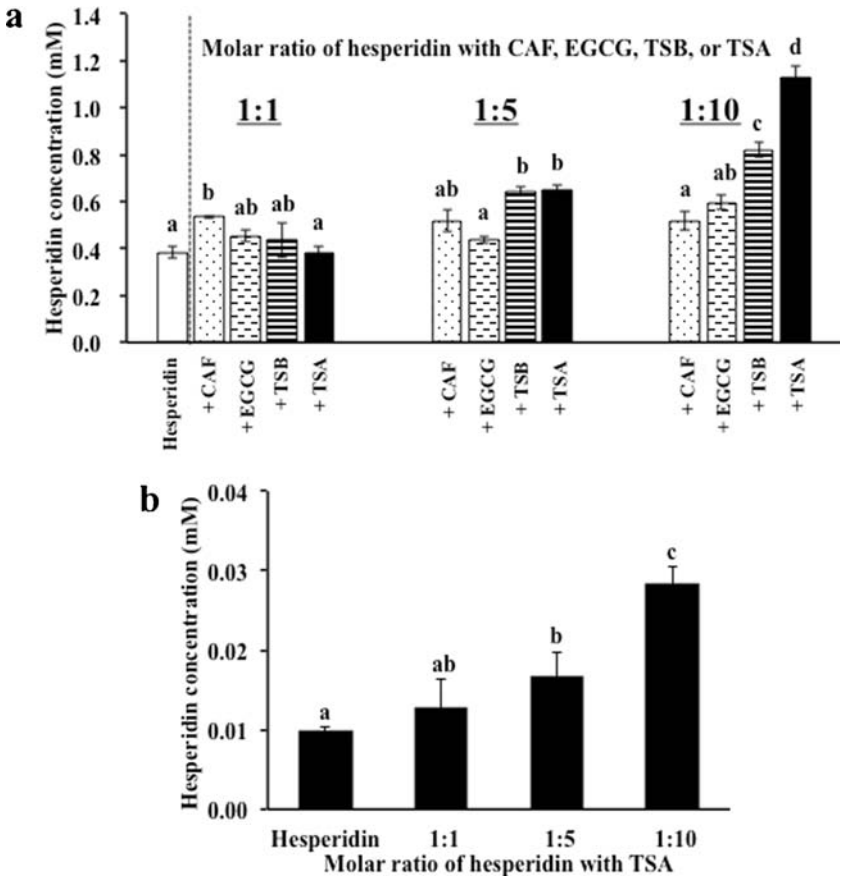

Fig. 2 Solubility of hesperidin upon the addition of caffeine (Hesp-CAF), (−)-epigallocatechin-3-*O*-gallate (Hesp-EGCG), theasinensin B (Hesp-TSB), and theasinensin A (Hesp-TSA) at molar ratios of 1:1, 1:5, and 1:10 in 10% DMSO (**a**); solubility of hesperidin with TSA at molar ratios of 1:1, 1:5, and 1:10 in water (**b**). Concentration of hesperidin in 10% DMSO or water was determined by LC-TOF/MS. Data were expressed as the mean ± SD ($n=3$). Means without a common letter in all groups differed at $p<0.05$ by Tukey-Kramer's *t*-test.

^{1}H-NMR Analysis of Hesperidin-TSA Complex

The water-soluble flavonoid of narirutin, which is structurally similar to hesperidin (Fig. 1) was combined with TSA and subjected to ^{1}H-NMR analyses in 10% DMSO-d_6 and D_2O to verify whether NMR solvents affected the change in observed chemical shifts ($\Delta\delta$). As a result, a similar trend of increasing $\Delta\delta$ values of all narirutin protons with increasing TSA concentrations (1:1 to 1:10 molar ratios) was observed in both solvent systems (Electronic supplementary material), suggesting that subsequent NMR experiments of hesperidin-TSA could be performed in 10% DMSO-d_6. Figure 3a–k show the typical ^{1}H-NMR spectra of hesperidin-TSA as a function of TSA concentration (0 to 1:10 molar ratios) in 10% DMSO-d_6. Increasing up-field shifts of the hesperidin H2′, 5′, 6′, H6, H8, and H2 protons were observed in hesperidin-TSA, as compared to those of hesperidin alone. In addition, the singlet peak of H6 and H8 of hesperidin (Fig. 3a) was observed as two singlet peaks upon addition of TSA (Fig. 3b–k), suggesting that intermolecular interactions between the aglycone moiety of hesperidin and TSA might have occurred. As shown in Fig. 4, marked up-field shifts in the $\Delta\delta$ of hesperidin upon addition of TSA were observed for H2 (0.05 to 0.27 ppm) and H2′, 5′, 6′ (0.03 to 0.19 ppm), indicating that the B-ring of

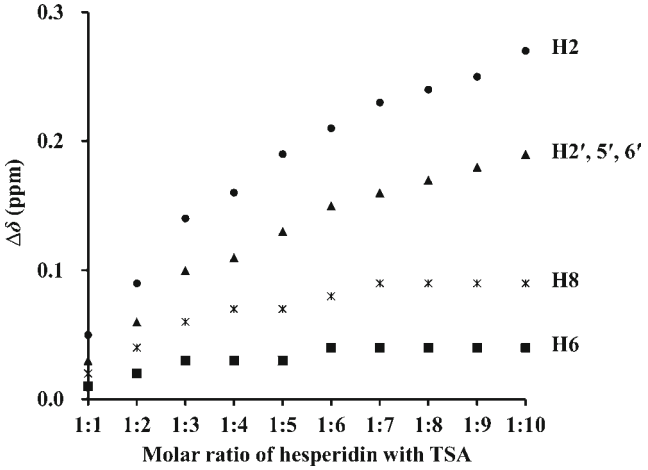

Fig. 4 Change in chemical shift ($\Delta\delta$, ppm) of hesperidin protons upon complexation with theasinensin A (TSA) at molar ratios of 1:1 to 1:10 in 10% DMSO-d_6 at 25°C. The $\Delta\delta$ was calculated by the difference between δ value of hesperidin alone and that of hesperidin complexed with TSA. Target protons of hesperidin were H2, H2′, 5′, 6′, H8, and H6.

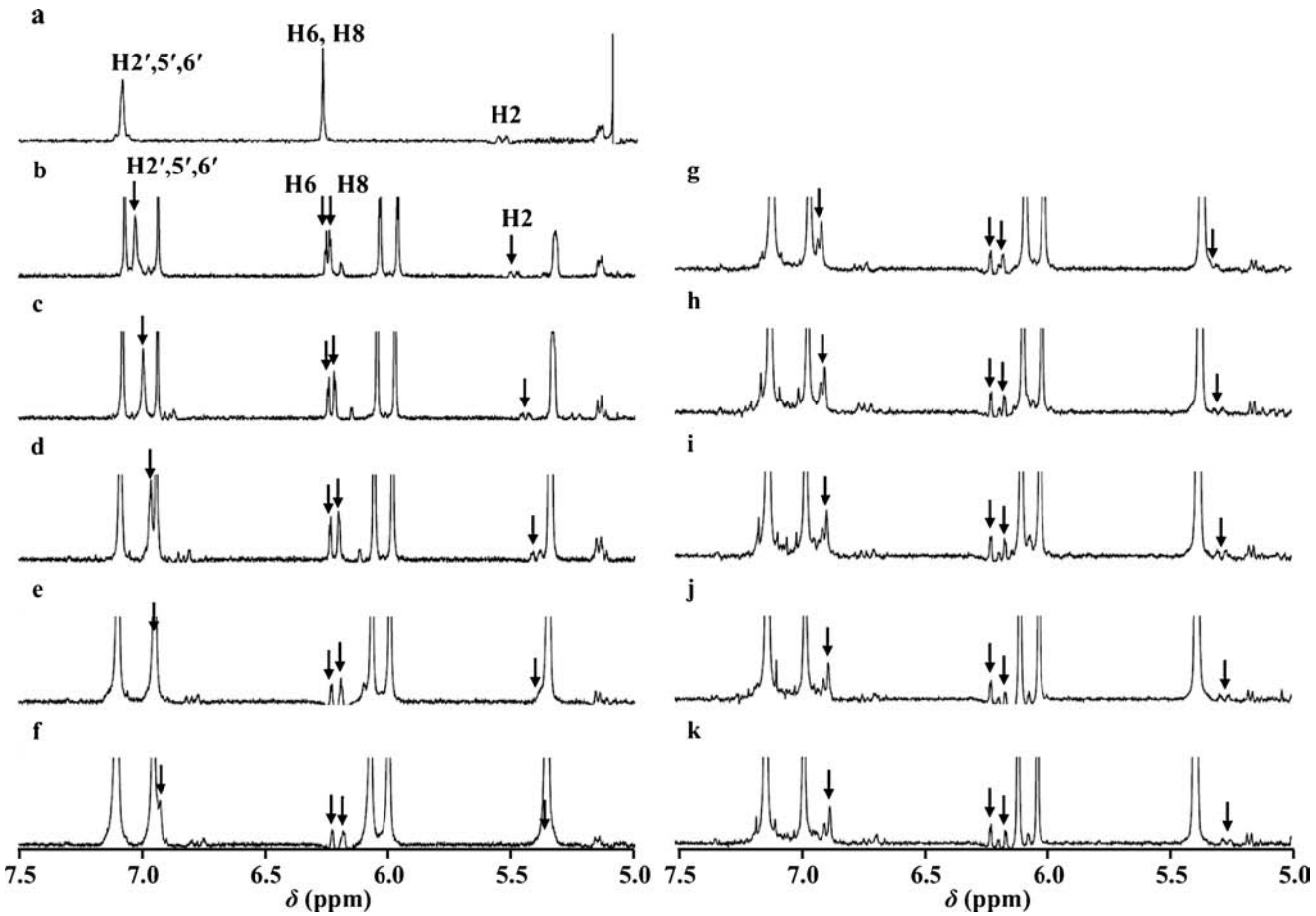

Fig. 3 ^{1}H-NMR spectra (5.0–7.5 ppm) of hesperidin alone (**a**) and a mixture of hesperidin and theasinensin A at molar ratios of 1:1 to 1:10 (**b**–**k**) in 10% DMSO-d_6 at 25°C. Target protons of hesperidin were H2′, 5′, 6′, H6, H8, and H2.

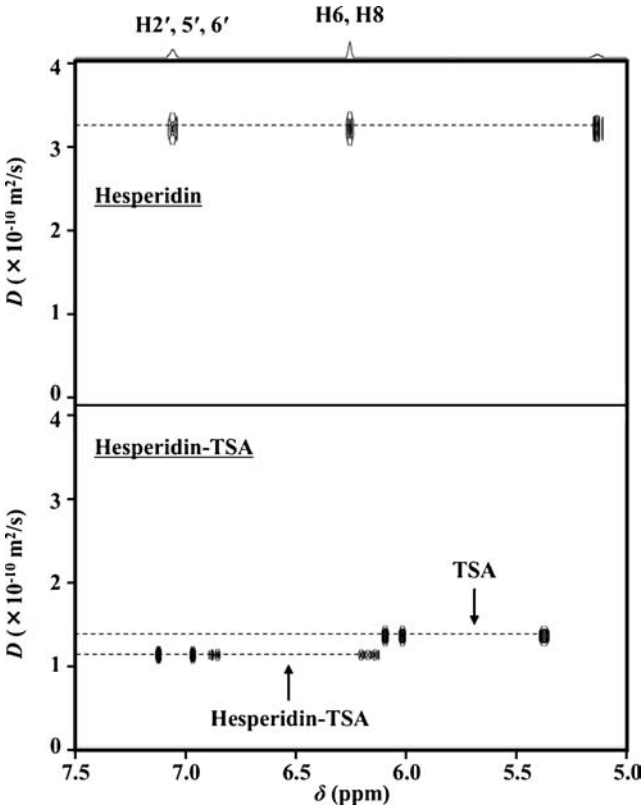

Fig. 5 DOSY-NMR spectra of hesperidin alone and complex with theasinensin A (TSA) in 10% DMSO-d_6. The *bottom* spectrum shows a mixture of hesperidin and TSA at molar ratio of 1:10.

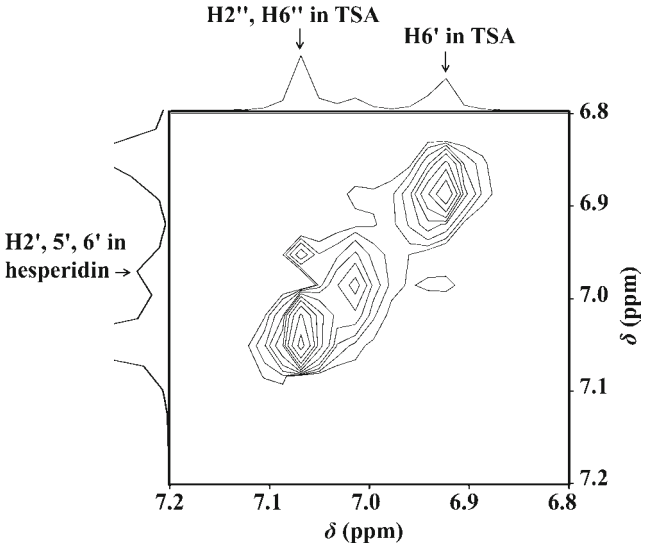

Fig. 6 Partial contour plot (6.8–7.2 ppm) of ROESY spectrum of hesperidin complexed with theasinensin A at molar ratio of 1:1 in 10% DMSO-d_6 at 25°C.

hesperidin might be associated with the enhanced solubility of hesperidin upon addition of TSA.

DOSY-NMR Analysis of Hesperidin-TSA Complex

To elucidate the complex formation between hesperidin and TSA, the change in the *D* value of hesperidin was utilized as an index in DOSY-NMR (Fig. 5). The *D* value of hesperidin was determined using the targeted single resonance signal from H2′, 5′, and 6′ (Fig. 3) normalized to that of the IS, DSS-d_6. As summarized in Table I, the *D* value of hesperidin dramatically decreased with increasing TSA concentrations (1.21 to 0.66×10^{-10} m^2/s), as compared to that of hesperidin alone (1.88×10^{-10} m^2/s). This clearly indicated that hesperidin and TSA formed a stable and larger complex in 10% DMSO solution.

ROESY-NMR Analysis of Hesperidin-TSA Complex

To determine the geometry of the hesperidin-TSA complex, ROESY-NMR was performed. As shown in Fig. 6, the ROESY spectrum revealed a significant intermolecular ROE correlation between H2′, 5′, and 6′ of hesperidin and H2″, 6″, and H6′ of TSA, while no cross peaks were observed for H2, H6, and H8 protons of hesperidin. This suggested that the B ring of hesperidin may be positioned near the B and/or G ring of TSA.

Theoretical Analysis of Hesperidin-TSA Complex

By considering the NMR-guided spatial configuration, which suggested that the intermolecular interactions between the B ring in hesperidin and the B and G rings in

Table I Diffusion Coefficients (*D*) of Hesperidin Complexed with Theasinensin A in 10% DMSO-d_6 by DOSY-NMR

Molar ratio of Hesp-TSA	1:0	1:1	1:2	1:3	1:4	1:5	1:6	1:7	1:8	1:9	1:10
D ($\times10^{-10}$ m^2/s)	1.88	1.21	0.78	0.58	0.67	0.56	0.65	0.63	0.58	0.65	0.66
ΔD	–	0.66	1.10	1.29	1.20	1.32	1.23	1.24	1.30	1.23	1.21

D value was normalized to that of DSS-d_6. The ΔD was obtained by the *D* value of hesperidin alone minus that of the hesperidin-theasinensin A complex (Hesp-TSA). DOSY-NMR measurements were performed using the spin-echo method at a field gradient pulse between 1.0×10^{-4} and 5.0×10^{-1} T/m at 25°C. The molar ratio of Hesp-TSA was 1:0 to 1:10

TSA (Fig. 6) may be involved in the enhanced solubilization of hesperidin by TSA, QM calculations of the hesperidin-TSA complex in water were carried out by computational simulations. As shown in Fig. 7a and b, both hesperidin and TSA were successfully optimized in the virtual water system; TSA was predicted to form a symmetrical conformation of two monomeric EGCG skeletons (Fig. 7a). Based on the ROESY result (Fig. 6), we proposed a 1:1 or 2:1 complex formation between hesperidin and TSA (Fig. 7c and d, respectively). The calculated ΔG value of the hesperidin-TSA complex suggested that complex formation occurred between two hesperidin molecules and one TSA molecule (ΔG of −23.5 kJ/mol), rather than between one hesperidin with TSA (Fig. 7c–e).

DISCUSSION

In an attempt to clarify the underlying mechanism of the enhanced solubility of water-insoluble hesperidin by tea polyphenols, the interactions between four typical tea polyphenols (CAF, EGCG, TSB, and TSA) and hesperidin were investigated in water. LC-TOF/MS analysis suggested a 3-fold enhancement in hesperidin solubility upon addition of TSA, indicating that TSA, an EGCG dimer, may be the primary constituent of black tea implicated in the enhanced solubility of hesperidin. Considering that the free galloly group(s) in catechins played a role in complex formation with CD (22), the two galloyl groups in TSA may also be involved in the enhanced solubility of hesperidin (Fig. 2).

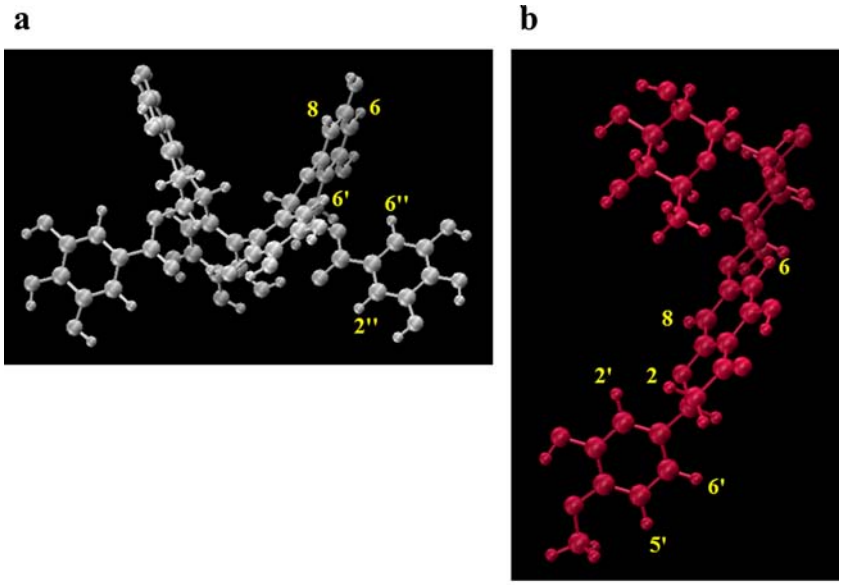

e

Hesperidin	TSA	Distance (Å)
H2'	H6'	4.5-4.6
H2'	H2''	4.9-5.0
H5'	H2''	5.0-6.0
H6'	H2''	5.0-6.0

Complex of hesperidin and TSA	ΔG (kJ/mol)
1:1	-10.0
2:1	-23.5

Fig. 7 Conformations of theasinensin A alone (**a**), hesperidin alone (**b**), the 1:1 complex (**c**), and 2:1 complex (**d**) of hesperidin and theasinensin A (TSA). The proton-proton interactions are indicated by the *yellow dotted line*. Distance (Å) between hesperidin and TSA, and ΔG (kJ/mol) of the 1:1 and 2:1 complexes (**e**).

^{1}H-, DOSY-, and ROESY-NMR shed light on the structural aspects of the enhanced solubility of hesperidin by TSA. Pescitelli *et al.* (23) revealed the benefits of these techniques in assessing intermolecular interactions in complexes *via* combinatorial applications. Therefore, using these NMR techniques, we could attribute the enhanced solubility of water-insoluble hesperidin to intermolecular interactions between the B ring of hesperidin with the B and G rings of TSA. The involvement of the B ring of hesperidin in complex formation was also reported by Ficara *et al.* (24), who demonstrated that the solubility of hesperidin could be enhanced by addition of β-CD, owing to pi-pi interactions of the B ring of hesperidin with the hydrophobic cavity of β-CD. A similar enhancement for improved drug solubility was observed with hydrophobic compounds, owing to pi-pi interactions (25), as the heterocyclic moiety of nicotinamide improved the solubility of an insoluble drug, diazepam, by promoting stacking interactions.

In order to clarify the configuration of the hesperidin-TSA complex, QM calculations were carried out. As previously reported (26, 27), computational analysis including QM and molecular docking simulations of ligand-protein interactions can support experimental findings regarding ligand bioactivity such as enzyme inhibition. The complex formed between catechin and β-CD was predicted by Jullian *et al.* (28), using semiempirical PM3 molecular docking simulations, as they revealed that the preferred location of the B ring of catechin was in the primary rim of β-CD. Considering the results obtained with ROESY-NMR (Fig. 6) and an X-ray crystallographic analysis of a crystalline gallocatechin-3-*O*-gallate (GCG)-CAF complex formed *via* pi-pi-interactions between the B and G rings of GCG and CAF (29), for the QM calculations we presumed that a space formed from the B and G rings of TSA might be a potential binding site for hesperidin. Our theoretical result (shown in Fig. 7) clearly indicated that 1:1 and 2:1 complexes of hesperidin and TSA positioned in the space between the B and G rings of TSA and hesperidin had negative ΔG values. The result that the 2:1 complex exhibited a higher ΔG value than the 1:1 complex also demonstrated that TSA could form complexes with hydrophobic compounds like hesperidin owing to the two symmetric spaces which were capable of pi-pi interaction. Lower enhanced solubility effect of TSB compared to TSA (Fig. 2a) might be due to its non-symmetric structure, and additional QM analysis for hesperidin-TSB complex must be needed. Notably the 1:2 complex between GCG and caffeine occurred owing to stacking interactions (29). However, the experimental results obtained regarding the solubility enhancement of hesperidin with increasing concentrations of TSA (Fig. 2) suggested that sandwich-like or stacking interactions between hesperidin and TSA in water must be involved in the enhanced solubilization of hesperidin at higher TSA concentrations, which was supported by the theoretical 2:1 complex of hesperidin and TSA (Fig. 7d).

CONCLUSION

For the first time, this study illustrated the complementarity of structural information obtained from NMR spectroscopy and theoretical analysis in the elucidation of the underlying mechanism of the enhanced solubility of hesperidin through a 2:1 complex formation with TSA. The present findings will increase the potential for the development and applications of water-insoluble bioactive natural compounds for alternative-medicinal food materials.

ACKNOWLEDGMENTS AND DISCLOSURES

This study was supported in part by Science and Technology Research Promotion Program for Agriculture, Forestry, Fisheries and Food Industry in Japan, and by Adaptable and Seamless Technology Transfer Program through target-driven R&D, JST in Japan. The authors have no conflicts of interest to declare.

REFERENCES

1. Garg A, Garg S, Zaneveld LJD, Singla AK. Chemistry and pharmacology of the citrus bioflavonoid hesperidin. Phytother Res. 2001;15(8):655–69.
2. Galati EM, Monforte MT, Kirjavainen S, Forestieri AM, Trovato A, Tripodo MM. Biological effects of hesperidin, a citrus flavonoid. (Note I): antiinflammatory and analgesic activity. Farmaco. 1994;40(11):709–12.
3. Borradaile NM, Carroll KK, Kurowska EM. Regulation of HepG2 cell apolipoprotein B metabolism by the citrus flavanones hesperetin and naringenin. Lipids. 1999;34(6):591–8.
4. Tanaka T, Makita H, Ohnishi M, Hirose Y, Wang A, Mori H, *et al.* Chemoprevention of 4-nitroquinoline 1-oxide-induced oral carcinogenesis by dietary curcumin and hesperidin: comparison with the protective effect of β-carotene. Cancer Res. 1994;54(4653):4653–9.
5. Hwang SL, Shih PH, Yen GC. Neuroprotective effects of citrus flavonoids. J Agric Food Chem. 2012;60(4):877–85.
6. Ishige K, Schubert D, Sagara Y. Flavonoids protect neuronal cells from oxidative stress by three distinct mechanisms. Free Radic Biol Med. 2001;30(4):433–46.
7. Gaur V, Kumar A. Hesperidin pre-treatment attenuates NO-mediated cerebral ischemic reperfusion injury and memory dysfunction. Pharmacol Rep. 2010;62(4):635–48.
8. Gil JM, Rego AC. Mechanisms of neurodegeneration in Huntington's disease. Eur J Neurosci. 2008;27(11):2803–20.
9. Figueiras A, Sarraguca JMG, Carvalho RA, Pais AACC, Veiga FJB. Interaction of omeprazole with a methylated derivative of β-cyclodextrin: phase solubility, NMR spectroscopy and molecular simulation. Pharm Res. 2007;24(2):377–89.
10. Vallejo F, Larrosa M, Escudero E, Zafrilla MP, Cerda B, Boza J, *et al.* Concentration and solubility of flavanones in orange beverages affect their bioavailability in humans. J Agric Food Chem. 2010;58(10):6516–24.
11. Kometani T, Terada Y, Nishimura T, Takii H, Okada S. Transglycosylation to hesperidin by cyclodextrin glucanotransferase from an alkalophilic *Bacillus* species in alkaline pH and properties of

hesperidin glycosides. Biosci Biotechnol Biochem. 1994;58(11): 1990–4.
12. Majumdar S, Srirangam R. Solubility, stability, physicochemical characteristics and *in vitro* ocular tissue permeability of hesperidin: a natural bioflavonoid. Pharm Res. 2009;26(5): 1217–25.
13. Nakayama H, Tanaka T, Miyata Y, Saito Y, Matsui T, Aramaki S, *et al*. Development of soluble hesperidin-containing fermented tea made from unripe mandarin orange fruits and third crop green tea leaves. J Jpn Soc Nutr Food Sci. 2014;67(2):95–103.
14. Shii T, Miyamoto M, Matsuo Y, Tanaka T, Kouno I. Biomimetic one-pot preparation of a black tea polyphenol theasinensin A from epigallocatechin gallate by treatment with copper (II) chloride and ascorbic acid. Chem Pharm Bull. 2011;59(9):1183–5.
15. Shii T, Tanaka T, Watarumi S, Matsuo Y, Miyata Y, Tamaya K, *et al*. Polyphenol composition of a functional fermented tea obtained by tea-rolling processing of green tea and loquat leaves. J Agric Food Chem. 2011;59(13):7253–60.
16. Caligiani A, Acquotti D, Palla G, Bocchi V. Identification and quantification of the main organic components of vinegars by high resolution ^{1}H NMR spectroscopy. Anal Chim Acta. 2007;585(1):110–9.
17. Cao R, Komura F, Nonaka A, Kato T, Fukumashi J, Matsui T. Quantitative analysis of D-(+)-glucose in fruit juices using diffusion ordered-^{1}H nuclear magnetic resonance spectroscopy. Anal Sci. 2014;30(3):383–8.
18. Cao R, Nonaka A, Komura F, Matsui T. Application of diffusion ordered-^{1}H-nuclear magnetic resonance spectroscopy to quantify sucrose in beverages. Food Chem. 2015;171(3):8–12.
19. Lucas LH, Otto WH, Larive CK. The 2D-J-DOSY experiment: resolving diffusion coefficients in mixtures. J Magn Reson. 2002;156(1):138–45.
20. Yanai T, Tew DP, Handy NC. A new hybrid exchange-correlation functional using the Coulomb-Attenuating Method (CAM-B3LYP). Chem Phys Lett. 2004;393(1–3):51–7.
21. Tomasi J, Mennucci B, Cammi R. Quantum mechanical continuum solvation models. Chem Rev. 2005;105(8):2999–3093.
22. Cai Y, Gaffney SH, Lilley TH, Magnolato D, Martin R, Spencer CM, *et al*. Polyphenol interactions. Part 4. Model studies with caffeine and cyclodextrins. J Chem Soc Perkin Trans. 1990;2(12):2197–209.
23. Pescitelli G, Bilia AR, Bergonzi MC, Vincieri FF, Di Bari L. Cyclodextrins as carriers for kavalactones in aqueous media: spectroscopic characterization of (*S*)-7,8-dihydrokavain and β-cyclodextrin inclusion complex. J Pharm Biomed Anal. 2010;52(4):479–83.
24. Ficarra R, Tommasini S, Raneri D, Calabro ML, Di Bella MR, Rustichelli C, *et al*. Study of flavonoids/β-cyclodextrins inclusion complexes by NMR, FT-IR, DSC, X-ray investigation. J Pharm Biomed Anal. 2002;29(6):1005–14.
25. Rasool AA, Hussain AA, Dittert LW. Solubility enhancement of some water-insoluble drugs in the presence of nicotinamide and related compounds. J Pharm Sci. 1991;80(4):387–93.
26. Khan MTHK, Dedachi K, Matsui T, Kurita N, Borgatti M, Gambari R, *et al*. Dipeptide inhibitors of thermolysin and angiotensin I-converting enzyme. Curr Top Med Chem. 2012;12(16):1748–62.
27. Kumrungsee T, Saiki T, Akiyama S, Nakashima K, Tanaka M, Kobayashi Y, *et al*. Inhibition of calcium-calmodulin complex formation by vasorelaxant basic dipeptides demonstrated by *in vitro* and *in silico* analyses. Biochim Biophys Acta. 2014;1840(10):3073–8.
28. Jullian C, Miranda S, Zapata-Torres G, Mendizabal F, Olea-Azar C. Studies of inclusion complexes of natural and modified cyclodextrin with (+)-catechin by NMR and molecular modeling. Bioorg Med Chem. 2007;15(2):3217–24.
29. Tsutsumi H, Sato T, Ishizu T. Stereochemical structure and intermolecular interaction complexes of (-)-gallocatechin-3-*O*-gallate and caffeine. Chem Pharm Bull. 2011;59(1):100–5.